

## Supplemental files

### Experimental section

#### Catalyst synthesis

The Ru/ZrO<sub>2</sub> catalyst was prepared by a spontaneous deposition method. Initially, zirconyl nitrate (0.05 mol), acetic acid (0.05 mol), deionized water (40 mL), and ethanol (120 mL) were mixed and stirred at 60 °C to yield a transparent solution and the mixture was continuously stirred for 0.5 h. Subsequently, formamide (0.1 mol) was added to this solution, and then epoxypropane (0.6 mol) was also added into this solution after stirred for another 0.5 h. Continued stirring for 0.5 h, the obtained gel was aged at 60 °C for 12 h. After mashed this gel, 0.12 g ruthenium(III) chloride (RuCl<sub>3</sub>) was added and continue stirring for 2 h. Afterward, the sample was centrifuged to remove the impurity and soaked in the ethanol for 48 h. Then obtained sample separated by centrifugation and dried at 60 °C. The product was calcined at 600 °C for 3 h at the air atmosphere. The catalyst was denoted as Ru/ZrO<sub>2</sub>.

The Ru/ZrO<sub>2</sub>@SiO<sub>2</sub> catalyst was also prepared by a spontaneous deposition method of protective shell. The difference is the gel was soaked in the tetraethyl orthosilicate (TEOS) solution rather than the ethanol. The catalyst was denoted as Ru/ZrO<sub>2</sub>@SiO<sub>2</sub>.

#### Catalyst characterizations

The X-ray diffraction (XRD) patterns of the Ru-Zr catalysts were performed on a SmartLab X-ray Diffractometer (Rigaku Corporation, Japan).

X-ray photoelectron spectrometer using the light source for Al K $\alpha$  (1486.6 eV) and 20 eV energy resolution. The experimental data were calibrated with the standard binding energy position C1s spectrum at 284.6 eV as a benchmark calibration.

The nitrogen adsorption and desorption isotherms was carried out on BEL sorp II apparatus. Before adsorption, the Ru-Zr samples were outgassed in vacuum at 200 °C. The surface area was determined by the BET theory. And the pore size was calculated by the BJH method.

The high resolution TEM images (HRTEM) were recorded using a JEOL JEM-2100 electron microscope.

The temperature-programmed reduction of H<sub>2</sub> (H<sub>2</sub>-TPR) was carried on the AutoChemII 2920 instrument. Firstly, the catalysts were pretreated under Ar flow at 200 °C for 1 h. Then the temperature was cooled to 50 °C, the catalyst was heated from 50 °C to 900 °C under 10 vol.% H<sub>2</sub>/Ar flow. The consumption of H<sub>2</sub> was detected by thermal conductivity detector (TCD).

Temperature-programmed desorption of C<sub>2</sub>H<sub>4</sub>Cl was investigated by AutoChem II 2920 apparatus. Prior to each test, the catalyst (50 mg, 40-60 meshes) was pretreated under high purified He at 200 °C for 1 h, then cooled down to 50 °C. After the catalyst was treated in toluene (1000 ppm)/He (30 mL·min<sup>-1</sup>) for 1 hour, it was purged with He gas for 0.5 hours. Finally, the system was heated to 600 °C at a heating rate of 10 °C·min<sup>-1</sup>, and the desorption profiles were recorded under He flow.

Temperature-programmed desorption of NH<sub>3</sub> (NH<sub>3</sub>-TPD) was investigated by AutoChem II 2920 apparatus. Prior to each test, the catalyst (50 mg, 40-60 meshes) was pretreated under high purified He at 200 °C for 1 h, then cooled down to 50 °C, and turned the flow of 10 vol% NH<sub>3</sub>/He into the system with a flow rate of 30 mL·min<sup>-1</sup> for 1 h. After that, the catalyst was flushed with He to remove physically adsorbed NH<sub>3</sub> on the catalyst surface. Finally, the system was heated to

500 °C at a heating rate of 10 °C·min<sup>-1</sup>, and the desorption profiles were recorded under He flow. The Py-IR was performed using Nicolet IS50 FTIR spectrometer. The Ru-Zr catalysts were pretreated at 200 °C for 1 h under vacuum, and a background spectrum was collected at 200 °C. Following the injection of pyridine at room temperature, the sample cell was saturated for 5 min, and then evacuated for 0.5 h under vacuum.

### Catalytic test

Catalytic oxidation reactions were carried out in a continuous flow fixed bed reactor constituted of a quartz tube of 20 mm of inner diameter at atmospheric pressure. 1g catalyst (16-40 meshes) mixing with 5 g quartz sand was placed at the middle of the quartz tube. The feed flow through the reactor was set at 250 mL·min<sup>-1</sup> and the space velocity (GHSV) was maintained at 15,000 h<sup>-1</sup>. The concentration of DCE in the reaction feeds was set at 1000 ppm. To study the effect of water on catalytic process, 5 vol % H<sub>2</sub>O was added into the system. In order to minimize the possible adsorption of the DCE on the inner surface of piping, the piping was heated by a heater band. The temperature of the reactor was measured with a thermocouple and the effluent gases were analyzed by an on-line gas chromatograph equipped with a flame ionization detector (FID). Catalytic activity was measured over the range 100-400°C and conversion data were calculated by the difference between inlet and outlet concentrations. HCl and Cl<sub>2</sub> were both trapped at the exit of the reactor in a bubbler containing an aqueous solution of KI. The concentrations of Cl<sub>2</sub> were calculated by titration with sodium thiosulfate (Na<sub>2</sub>S<sub>2</sub>O<sub>3</sub>) using starch as indicator. And the concentrations of HCl were calculated by titration with sodium hydroxide (NaOH) using phenolphthalein as indicator. The HCl selectivity was calculated according to the following equations (C<sub>x</sub>H<sub>y</sub>Cl<sub>z</sub> represents to the byproducts that may arise from the inadequacy decomposition of the reactant).

$$DCE\ Conversion(\%) = \frac{C_{in} - C_{out}}{C_{in}} \times 100\%$$

$$S_{HCl}(\%) = \frac{[HCl]_{out}}{[HCl]_{out} + 2[Cl_2]_{out} + z[C_xH_yCl_z]_{out}} \times 100\%$$

### In-situ FTIR study

*In-situ* FTIR spectra were performed on an *in situ* FTIR spectrometer (IS50) equipped with an *in-situ* cell. The sample was pressed into the *in-situ* cell and pretreated at 500 °C for 1 h under N<sub>2</sub> stream. Subsequently, the temperature was cooled down, and the infrared spectrum as the background was collected. Eventually, 100 mL·min<sup>-1</sup> (1000 ppm DCE, 20 vol% O<sub>2</sub> and N<sub>2</sub> as balance gas) gas mixture was introduced into the *in-situ* cell, and the spectra were recorded by accumulating 32 scans at spectral resolution of 4 cm<sup>-1</sup>.

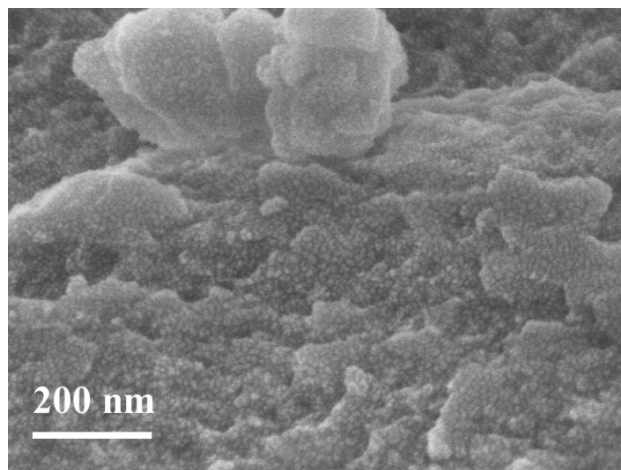


Fig. S1 The SEM images of Ru/ZrO<sub>2</sub>@SiO<sub>2</sub> catalyst.

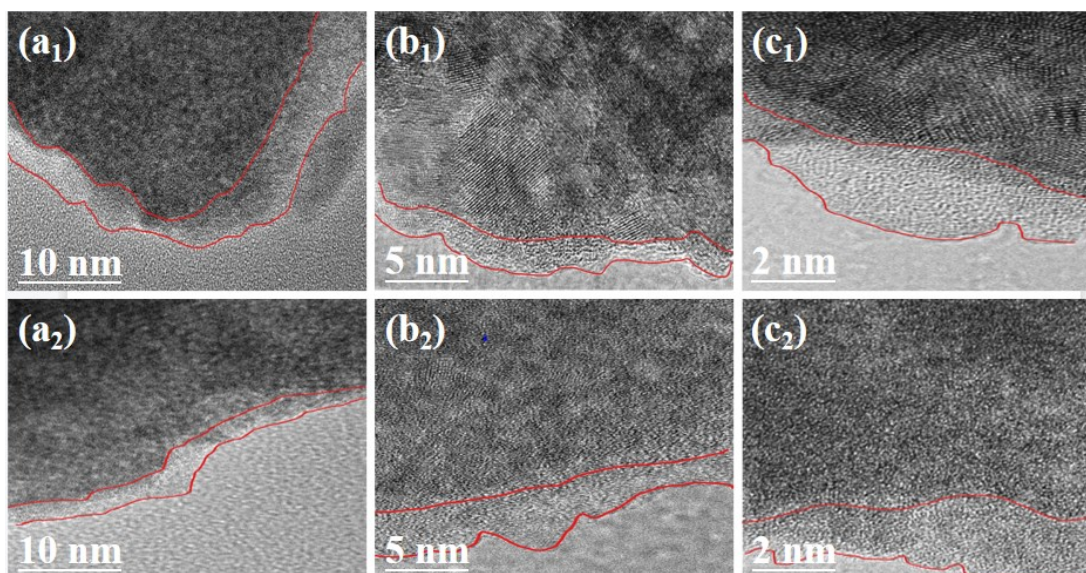


Fig. S2 The TEM images of Ru/ZrO<sub>2</sub>@SiO<sub>2</sub> catalysts.

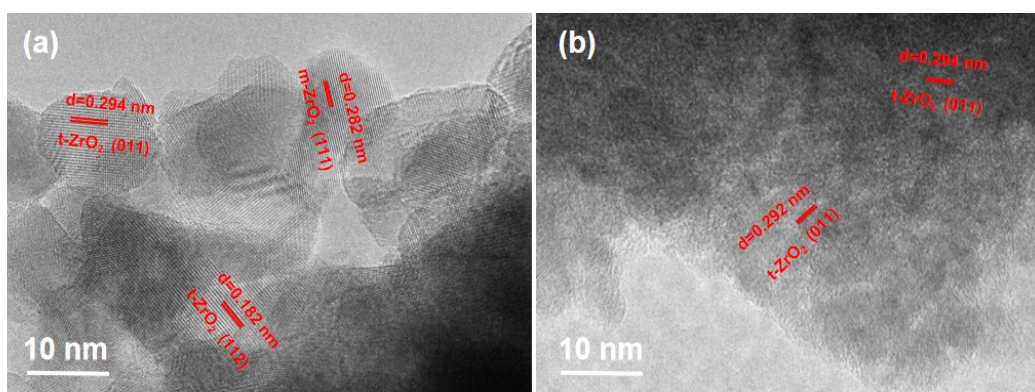


Fig. S3 The TEM images of (a) Ru/ZrO<sub>2</sub> and (b) Ru/ZrO<sub>2</sub>@SiO<sub>2</sub> catalysts.

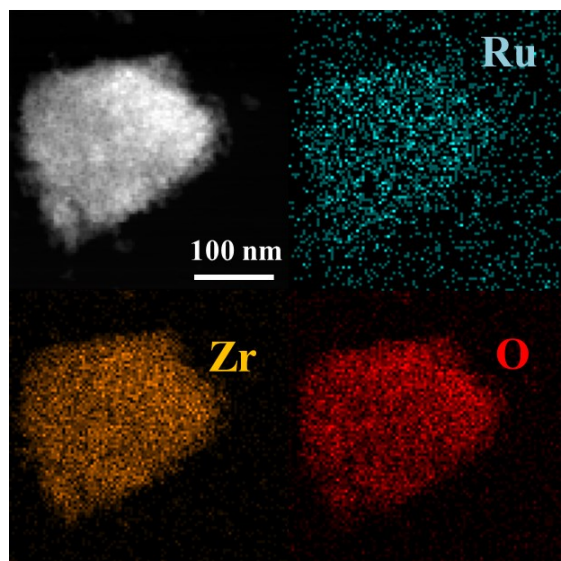


Fig. S4 The STEM HAADF images and EDX elemental mapping of Ru/ZrO<sub>2</sub> catalyst.

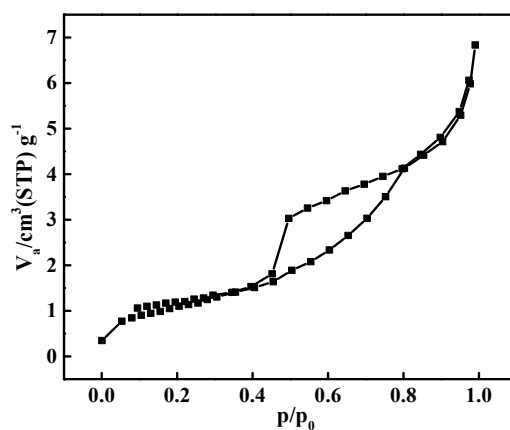


Fig. S5 N<sub>2</sub> adsorption-desorption isotherms of Ru/ZrO<sub>2</sub> catalyst.

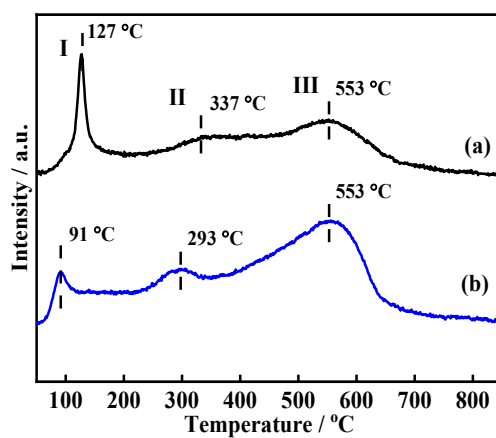


Fig. S6 The H<sub>2</sub>-TPR profiles of (a) Ru/ZrO<sub>2</sub>@SiO<sub>2</sub> and (b) Ru/ZrO<sub>2</sub> catalysts.

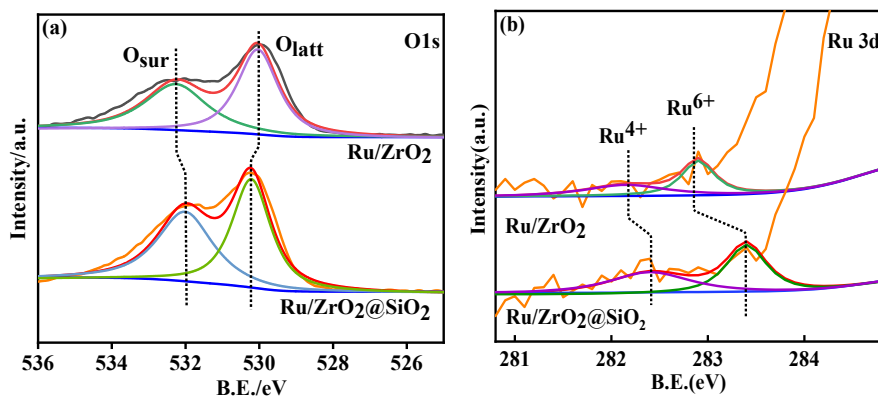


Fig. S7 The XPS spectra of Ru/ZrO<sub>2</sub>@SiO<sub>2</sub> and Ru/ZrO<sub>2</sub> catalysts: (a) O 1s, (b) Ru 3d.

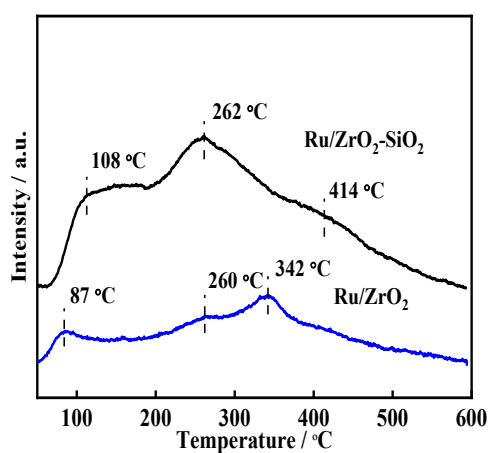


Fig. S8 The NH<sub>3</sub>-TPD of Ru/ZrO<sub>2</sub>@SiO<sub>2</sub> and Ru/ZrO<sub>2</sub> catalysts.

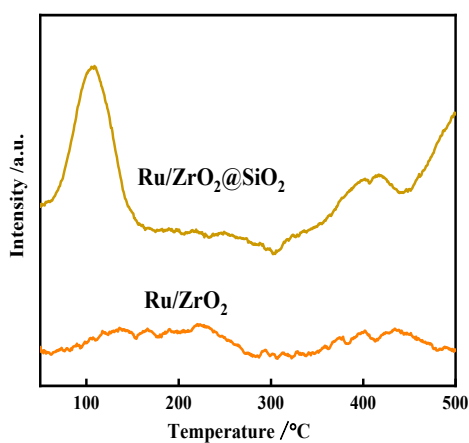


Fig. S9 The C<sub>2</sub>H<sub>4</sub>Cl<sub>2</sub>-TPD of Ru/ZrO<sub>2</sub>@SiO<sub>2</sub> and Ru/ZrO<sub>2</sub> catalysts.

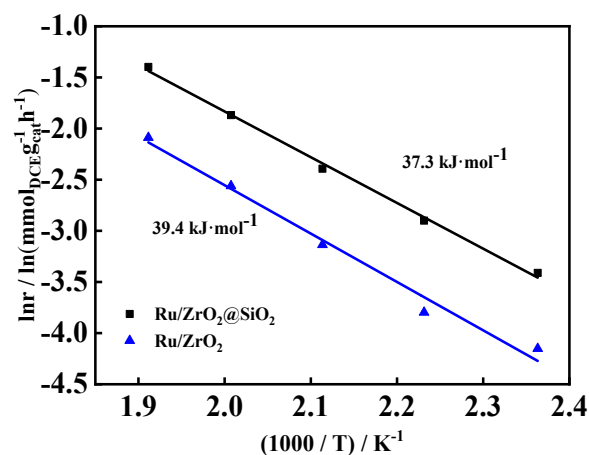


Fig. S10 The Arrhenius plots of DCE combustion over Ru/ZrO<sub>2</sub>@SiO<sub>2</sub> and Ru/ZrO<sub>2</sub> catalysts.

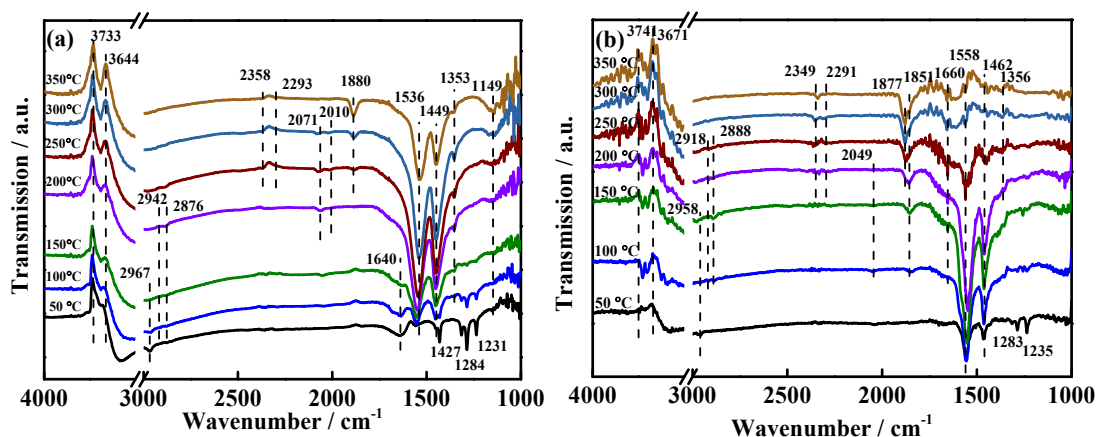


Fig. S11 *In-situ* FTIR spectra of DCE oxidation over Ru-Zr catalysts: (a) Ru/ZrO<sub>2</sub>@SiO<sub>2</sub>, (b) Ru/ZrO<sub>2</sub>.

The bands at 1231, 1284, 1427 and 2967 cm<sup>-1</sup> assigning to  $\tau$ CH<sub>2</sub>,  $\omega$ CH<sub>2</sub>,  $\delta$ CH<sub>2</sub>,  $\nu_s$ CH<sub>2</sub> of DCE were observed at 50 °C (Fig S11 (a)),<sup>1</sup> indicating that DCE molecules were adsorbed on hydroxyl groups of Ru/ZrO<sub>2</sub>@SiO<sub>2</sub> catalyst. The band at around 1640 cm<sup>-1</sup> can be attributed to  $\nu$ (C=C),<sup>2</sup> which hinted the formation of the byproduct vinyl chloride. When the temperature rose to 100 °C, two new bands at around 2942 and 2876 cm<sup>-1</sup> were monitored, which would be attributed to the CH<sub>3</sub>- stretching vibration. The weak bands at 1149 cm<sup>-1</sup> corresponding to  $\rho$ (CH<sub>3</sub>) vibrational modes of chlorinated ethoxy.<sup>3</sup> In addition, the bands at 1536 and 1449 cm<sup>-1</sup> represent asymmetric/symmetric stretching of the carboxylate (COO<sup>-</sup>).<sup>4</sup> It can be concluded that VC was oxidized to CH<sub>3</sub>COOH. When the temperature rose to 200 °C, the some peaks were monitored that those at 2071 and 2010 cm<sup>-1</sup> attributed to CO and could be ascribed to carbonates at 1353 cm<sup>-1</sup>. The band related to CO<sub>2</sub> (2358 and 2293 cm<sup>-1</sup>) started to evolve at 250 °C and it was enhanced by increasing the temperature. At high temperature, the bands around 1850 cm<sup>-1</sup> were commonly regarded as stretching vibrations of C=O for anhydride (O=C-O-C=O, 1880 cm<sup>-1</sup>), acyl chloride (O=CCl, 1858 cm<sup>-1</sup>) which were attributed to the polychlorinated by-products formed.<sup>5</sup>

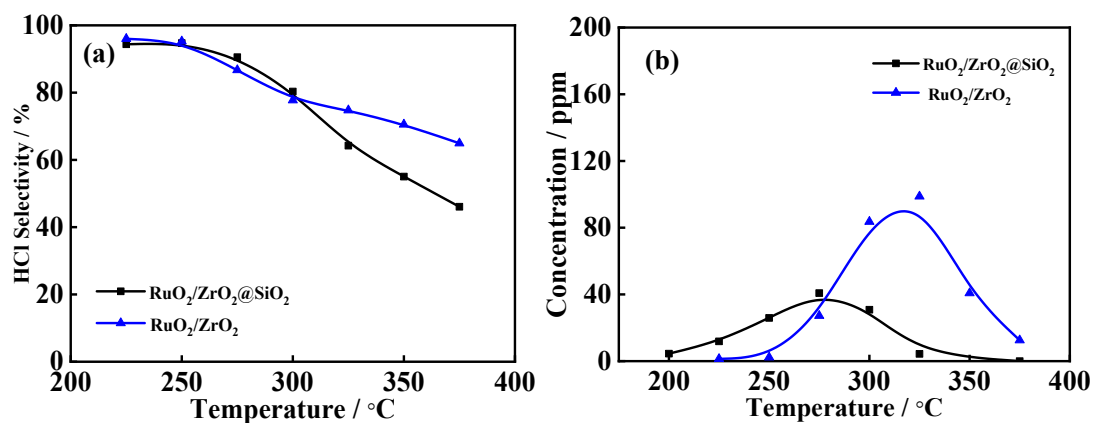


Fig. S12 The (a) HCl selectivity and (b) concentration of the VC.

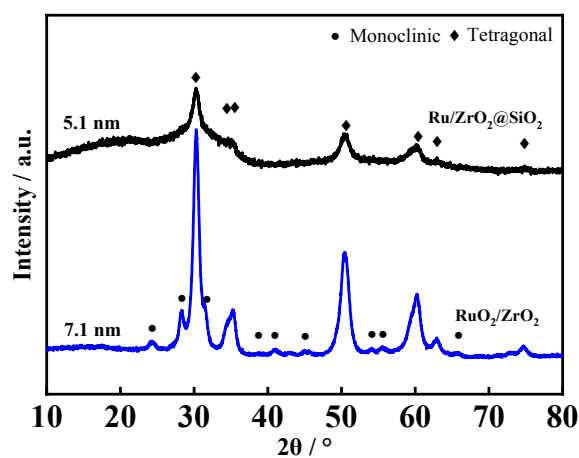
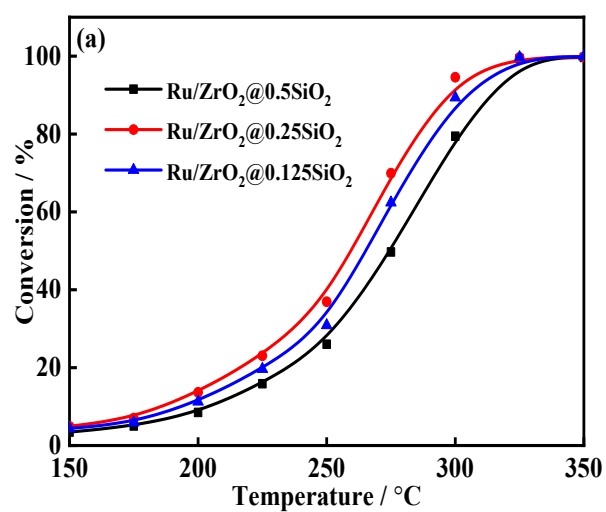
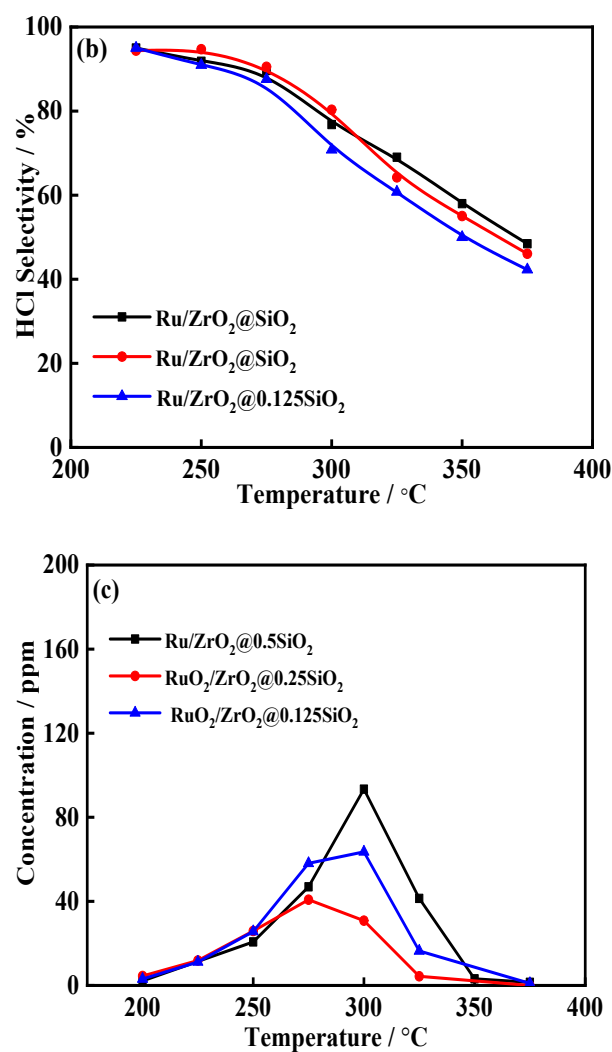


Fig. S13 XRD patterns of the used Ru/ZrO<sub>2</sub>@SiO<sub>2</sub> and Ru/ZrO<sub>2</sub> catalysts.





**Fig. 14** The light-off curves of DCE combustion over Ru/ZrO<sub>2</sub>@SiO<sub>2</sub> catalysts. (a) DCE conversion, (b) HCl selectivity, (c) the concentration of the VC.

**Tab. S1** The XPS results of Ru-Zr catalysts.

Catalysts	O <sub>sur</sub> <sup>a</sup> /%	O <sub>latt</sub> <sup>b</sup> /%	Ru <sup>4+</sup> /%	Ru <sup>6+</sup> /%
Ru/ZrO <sub>2</sub>	41.8	58.2	42.7	57.3
Ru/ZrO <sub>2</sub> @SiO <sub>2</sub>	47.9	52.1	46.5	53.5

a. the surface adsorbed oxygen.

b. the surface lattice oxygen.

**Tab. S2** The reaction data for DCE oxidation over Ru-Zr catalysts.

Catalysts	Ru <sup>a</sup> / wt%	Reaction condition <sup>b</sup>	T <sub>50</sub> <sup>c</sup> / °C	T <sub>90</sub> <sup>c</sup> / °C	Specific rate <sup>d</sup> / mmol·g <sub>Ru</sub> <sup>-1</sup> ·h <sup>-1</sup>	Ref.
Ru/ZrO <sub>2</sub> @SiO <sub>2</sub>	0.52	SV=15000 h <sup>-1</sup>	260	297	1.17	This work
Ru/ZrO <sub>2</sub>	0.54	SV=15000 h <sup>-1</sup>	291	328	0.71	This



						work
Ru/CeO <sub>2</sub>	1.81	SV=30000 h <sup>-1</sup>	325	386	0.35	[6]
Ru/Al <sub>2</sub> O <sub>3</sub>	1.78	SV=30000 h <sup>-1</sup>	299	328	0.38	[6]
Pt/CeO <sub>2</sub>	0.5	SV=15000 h <sup>-1</sup>	--	364	--	[7]
Pt/TiO <sub>2</sub>	0.5	SV=15000 h <sup>-1</sup>	--	375	--	[7]
Ru/HZSM-5	0.88	SV=20000 h <sup>-1</sup>	260	308	--	[8]
RuCo/HZSM-5	0.91	SV=20000 h <sup>-1</sup>	238	281	---	[8]
Ru/MgO	0.93	SV=20000 h <sup>-1</sup>	403	455	--	[8]

a. Determined by XRF or ICP.

b. The concentration of DCE in the reaction feeds was set at 1000 ppm.

c. The temperature of DCE conversion at 50 % and 90 %.

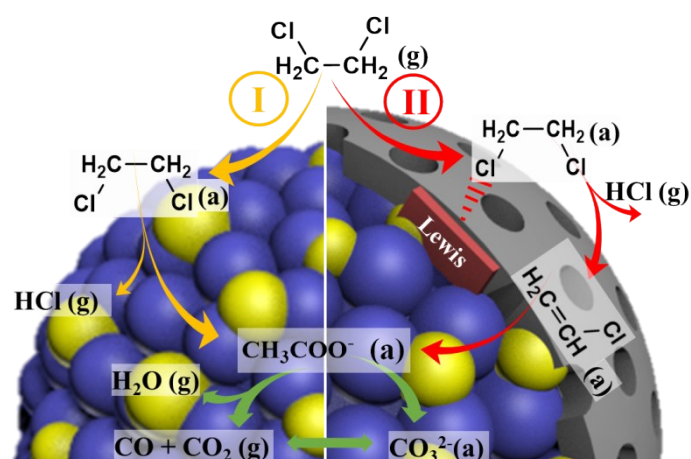
d. Specific activity per catalyst mass unit at 300 °C.

**Tab. S3** The reaction data for DCE oxidation over Ru-Zr catalysts.

Catalysts	T <sub>50</sub> <sup>a</sup> / °C	T <sub>90</sub> <sup>a</sup> / °C	Specific rate <sup>b</sup> / mmol·g <sub>Ru</sub> <sup>-1</sup> ·h <sup>-1</sup>	VC <sub>max</sub> / ppm	Ea / kJ·mol <sup>-1</sup>
Ru/ZrO <sub>2</sub> @0.5SiO <sub>2</sub>	274	314	1.08	93.39	38.00
Ru/ZrO <sub>2</sub> @0.25SiO <sub>2</sub>	260	297	1.17	40.78	37.18
Ru/ZrO <sub>2</sub> @0.125SiO <sub>2</sub>	262	301	1.12	63.54	37.34

a. The temperature of DCE conversion at 50 % and 90 %.

b. Specific activity per catalyst mass unit at 300 °C.



**Scheme S1.** Proposed mechanism for DCE oxidation of Ru-Zr catalysts

1. S. X. Bai, B. B. Shi, W. Deng, Q. G. Dai and X. Y. Wang, *RSC Adv.*, 2015, **5**, 48916-48927.
2. Q. G. Dai, L. L. Yin, S. X. Bai, W. Wang, X. Y. Wang, X. Q. Gong and G. Z. Lu, *Appl. Catal. B: Environ.*, 2016, **182**, 598-610.
3. S. X. Bai, Q. G. Dai, X. X. Chu and X. Y. Wang, *RSC Adv.*, 2016, **6**, 52564-52574.

4. P. Yang, Z. Meng, S. Yang, Z. Shi and R. Zhou, *J. Mol. Catal. Chem.*, 2014, **393**, 75-83.
5. X. L. Liu, J. L. Zeng, W. B. Shi, J. Wang, T. Y. Zhu and Y. F. Chen, *Catal. Sci. Technol.*, 2017, **7**, 213-221.
6. Y. F. Gu, X. X. Jiang, W. Sun, S. X. Bai, Q. G. Dai and X. Y. Wang, *ACS Omega*, 2018, **3**, 8460-8470.
7. Y. J. Shi, J. L. Wang and R. X. Zhou, *Chemosphere*, 2021, **265**, 8.
8. X. Zhang, L. Y. Dai, Y. X. Liu, J. G. Deng, L. Jing, Z. W. Wang, W. B. Pei, X. H. Yu, J. Wang and H. X. Dai, *Appl. Catal. B. Environ.*, 2021, **285**, 16.